

# Generic Contrast Agents

Our portfolio is growing to serve you better. Now you have a *choice*.



[VIEW CATALOG](#)

# AJNR

## Tractography of the Cerebellar Peduncles in Second- and Third-Trimester Fetuses

F. Machado-Rivas, O. Afacan, S. Khan, B. Marami, C.K. Rollins, C. Ortinau, C. Velasco-Annis, S.K. Warfield, A. Gholipour and C. Jaimes

This information is current as of May 4, 2025.

*AJNR Am J Neuroradiol* 2021, 42 (1) 194-200

doi: <https://doi.org/10.3174/ajnr.A6869>

<http://www.ajnr.org/content/42/1/194>

# Tractography of the Cerebellar Peduncles in Second- and Third-Trimester Fetuses

 F. Machado-Rivas,  O. Afacan,  S. Khan,  B. Marami,  C.K. Rollins,  C. Ortinau,  C. Velasco-Annis,  S.K. Warfield,  A. Gholipour, and  C. Jaimes



## ABSTRACT

**BACKGROUND AND PURPOSE:** Little is known about microstructural development of cerebellar white matter in vivo. This study aimed to investigate developmental changes of the cerebellar peduncles in second- and third-trimester healthy fetuses using motion-corrected DTI and tractography.

**MATERIALS AND METHODS:** 3T data of 81 healthy fetuses were reviewed. Structural imaging consisted of multiplanar T2-single-shot sequences; DTI consisted of a series of 12-direction diffusion. A robust motion-tracked section-to-volume registration algorithm reconstructed images. ROI-based deterministic tractography was performed using anatomic landmarks described in postnatal tractography. Asymmetry was evaluated qualitatively with a perceived difference of >25% between sides. Linear regression evaluated gestational age as a predictor of tract volume, ADC, and fractional anisotropy.

**RESULTS:** Twenty-four cases were excluded due to low-quality reconstructions. Fifty-eight fetuses with a median gestational age of 30.6 weeks (interquartile range, 7 weeks) were analyzed. The superior cerebellar peduncle was identified in 39 subjects (69%), and it was symmetric in 15 (38%). The middle cerebellar peduncle was identified in all subjects and appeared symmetric; in 13 subjects (22%), two distinct subcomponents were identified. The inferior cerebellar peduncle was not found in any subject. There was a significant increase in volume for the superior cerebellar peduncle and middle cerebellar peduncle (both,  $P < .05$ ), an increase in fractional anisotropy (both,  $P < .001$ ), and a decrease in ADC (both,  $P < .001$ ) with gestational age. The middle cerebellar peduncle had higher volume ( $P < .001$ ) and fractional anisotropy ( $P = .002$ ) and lower ADC ( $P < .001$ ) than the superior cerebellar peduncle after controlling for gestational age.

**CONCLUSIONS:** A robust motion-tracked section-to-volume registration algorithm enabled deterministic tractography of the superior cerebellar peduncle and middle cerebellar peduncle in vivo and allowed characterization of developmental changes.

**ABBREVIATIONS:** FA = fractional anisotropy; GA = gestational age; ICP = inferior cerebellar peduncle; MCP = middle cerebellar peduncle; MCP<sub>cog</sub> = cognitive pathway of middle cerebellar peduncle; MCP<sub>mot</sub> = motor pathway of middle cerebellar peduncle; MT-SVR = motion-tracked slice-to-volume registration; SCP = superior cerebellar peduncle

In the second half of pregnancy, the cerebellum is growing rapidly and is extremely vulnerable.<sup>1</sup> Despite the increasingly recognized association of antenatal and perinatal cerebellar injury with adverse motor and neurologic outcomes later in life,<sup>2-5</sup> little is known about normal cerebellar developmental in the later part of gestation, in particular with regard to changes in microstructure. In fact, most

existing fetal MR imaging data addresses primarily changes in cerebellar volume with gestational age (GA) or changes in volume and


Received May 11, 2020; accepted after revision August 24.


Computational Radiology Laboratory (F.M.-R., O.A., S.K., B.M., C.V.-A., S.K.W., A.G., C.J.), Department of Radiology, Department of Neurology (C.K.R.), and Fetal-Neonatal Neuroimaging and Developmental Science Center (C.J.), Boston Children's Hospital, Boston, Massachusetts; Harvard Medical School (F.M.-R., O.A., S.K., B.M., C.K.R., S.K.W., A.G., C.J.), Boston, Massachusetts; and Department of Pediatrics (C.O.), Washington University School of Medicine in St. Louis, St. Louis, Missouri.


The content is solely the responsibility of the authors and does not necessarily represent the official views of the National Institutes of Health, the Fetal Health Foundation or the McKnight Foundation.

Research reported in this study was supported, in part, by the American Academy of Neurology, grant/award No. ???????; a Clinical Research Training Fellowship; the Fetal Health Foundation; the McKnight Foundation; the National Alliance for Research on Schizophrenia and Depression, grant/award No. ???????; Young Investigator; National Heart, Lung, and Blood Institute, grant/award No. K23HL141602; Scholar Award from the Pediatric Heart Network; National Institute of Neurological Disorders and Stroke, grant/award No. K23NS101120; National Institutes of Health, grant/award Nos. R01EB013248, R01EB018988, R01NS106030; and a Schlaeger Fellowship for Neuroscience Research.

Please address correspondence to Camilo Jaimes, MD, Harvard Medical School, Boston, MA 02115; e-mail: camilo.jaimescobos@childrens.harvard.edu

 Indicates open access to non-subscribers at [www.ajnr.org](http://www.ajnr.org)

 Indicates article with supplemental on-line tables.

 Indicates article with supplemental on-line photo.

<http://dx.doi.org/10.3174/ajnr.A6869>

their association with specific diseases such as congenital heart disease.<sup>6-8</sup>

In vivo evaluation of cerebellar microstructure using fetal MR imaging has been limited by the technical challenges related to imaging the gravid abdomen, particularly patient motion. However, data from ex vivo MR imaging studies are promising. For instance, Takahashi et al<sup>9,10</sup> performed high-resolution ex vivo DTI of fetal specimens and demonstrated the feasibility of using tractography to outline the cerebellar peduncles prenatally. Even though tractography of the cerebellar peduncles has been sporadically reported in vivo in technical articles or general review articles on fetal DTI,<sup>11</sup> the GA-related microstructural changes that occur in the cerebellar peduncles in the second half of pregnancy remain largely unexplored.

Recent advances in hardware and software have improved fetal MR imaging substantially. The use of 3T magnets, which have been shown to be safe, results in improvement of the SNR and spatial resolution, which is advantageous to image the small structures of the fetal brain.<sup>12,13</sup> In addition, postprocessing algorithms that enable reconstruction of motion-corrected fetal DTI data are increasingly available and have been used by several groups to characterize the development of the supratentorial white matter tracts in vivo.<sup>14-16</sup> We hypothesize that fetal DTI performed at 3T and processed with a robust section-to-volume motion-correction and registration<sup>14</sup> algorithm will enable tractography of the cerebellar peduncles in fetuses in the second and third trimesters of pregnancy. We aimed to characterize fetal cerebellar tract microstructure and to investigate tract-specific developmental changes.

## MATERIALS AND METHODS

### Subjects

This was an institutional review board–approved and Health Insurance Portability and Accountability Act–compliant study. We performed a retrospective analysis of MR imaging data that were previously collected for a prospective study of normal fetal brain development in healthy pregnant volunteers and for a study on developmental abnormalities of the brain in fetuses with congenital heart disease.<sup>15,17</sup> Inclusion criteria for those studies were the following: 1) normal pregnancy on routine prenatal care, 1) maternal age 18–45 years, gestational age (GA) of at least 18 weeks, and 3) availability of fetal DTI data. Exclusion criteria were the following: 1) maternal contraindication to MR imaging, 2) known congenital infection in the fetus, 3) abnormalities in the fetus (known from prior clinical care, or detected during the research fetal MR imaging), 4) chromosomal abnormalities, and 5) multiple-gestation pregnancy. Only control subjects enrolled in the congenital heart disease study were eligible for our analysis. Pregnant volunteers were recruited through our institution's intranet and through pamphlets for participation in a research scan at various clinics. The informed consent process (which included a written informed consent form) was completed for each patient.

### Image Acquisition

Fetal MRIs were acquired on a 3T MR imaging scanner (Skyra or Prisma; Siemens) using an 18-channel body-array coil, without maternal breath-holding or sedation. Structural brain images were acquired with multiple T2-weighted HASTE scans in the

orthogonal plane with the following sequence parameters: TR = 1400–2000 ms, TE = 100–120 ms, 0.9- to 1.1-mm in-plane resolution, 2-mm thickness with no interslice space, acquisition matrix size = 256 × 204, 256 × 256, or 320 × 320 with a 2- or 4-section interleaved acquisition. Diffusion data were acquired with 2–8 scans in orthogonal planes with respect to the fetal head. The diffusion acquisitions included 1 or 2  $b = 0$  s/mm<sup>2</sup> images and 12 diffusion-sensitized images at  $b = 500$  s/mm<sup>2</sup> with TR = 3000–4000 ms, TE = 60 ms, in-plane resolution = 2 mm, and section thickness = 2–4 mm.

### Image Processing

Structural data were processed with an automated motion-robust fetal MR imaging volume-reconstruction algorithm that created a 3D isotropic intensity-normalized T2WI volume of the fetal brain from multiple HASTE scans.<sup>18</sup> Diffusion data were processed using a validated section-to-volume registration algorithm with a motion-trajectory-estimation framework, referred to as motion-tracked section-to-volume registration (MT-SVR).<sup>14,19</sup> Briefly, the MT-SVR does the following: 1) estimates the relative motion of the fetal brain for every diffusion-sensitized section using a state-space model and registering the section into a reference space, which is the reconstructed T2WI volume; 2) excludes data corrupted by intraslice motion; and 3) estimates the diffusion tensor at every voxel of the reference space using the motion-compensated data. For most subjects, 3–4 acquisitions in the coronal and axial planes were used to reconstruct DTI data. To perform tractography, we used the Diffusion Toolkit (Version 0.6.4.1; TrackVis; <http://www.trackvis.org/dtk/>). We used an angle threshold of 35° to stop tract propagation and an automatic fractional anisotropy (FA) mask threshold as determined by the Diffusion Toolkit.<sup>20</sup> A deterministic tractography with fiber assignment by continuous tracking approach with user-defined ROIs was used.

### Image Segmentation and Analysis

We reviewed data from 82 fetuses. The DTI sequences were performed in all subjects, independent of whether the fetus was active or whether other artifacts, such as ghosting or susceptibility, degraded the acquisitions. Before image segmentation for our study, we performed a visual quality-assessment inspection of the MT-SVR-processed data by reconstructing whole-brain tracts. If there were gross distortions on whole-brain tracts, the reconstruction was excluded from the analysis and designated as “low-quality” reconstruction.

The cerebellar peduncles were segmented by placing ROIs in anatomically relevant landmarks using a combination of T2WI reconstructed images and scalar diffusion maps (FA, ADC, and trace diffusion). A trained research fellow (F.M.-R.) placed ROIs that were subsequently reviewed by a pediatric neuroradiologist with experience in fetal imaging (C.J.). The selection of ROIs was based on the anatomic landmarks of previously published studies on cerebellar peduncle tractography by Catani et al<sup>21</sup> and used by Re et al.<sup>22</sup> Specifically, for the superior cerebellar peduncles (SCPs), the ROIs were placed in the cerebellar hemispheres and in the midbrain. The ROI in the cerebellar hemispheres was placed in a single coronal section, just posterior to the fastigial point, covering the entire area of the cerebellum. The ROI for the

midbrain was placed in the coronal plane, anterior to the insertion of the SCP and the cerebral aqueduct, encompassing the upper half of the midbrain. For the MCP, the ROIs were placed in the cerebellar hemispheres (same as above) and the pons. The ROI for the pons was placed in a single coronal section through the midpons, covering its entire SI dimension from the pontomesencephalic sulcus to the pontomedullary sulcus. For the inferior cerebellar peduncle (ICP), ROIs were placed in the cerebellar hemispheres and the medulla. The ROI for the medulla was placed in a single axial section at the level of the outlet of the fourth ventricle. All ROIs were drawn using TrackVis (Trackvis 0.6.1) (Online Figure).

To evaluate the outcome of the tractography, a pediatric neuro-radiologist visually inspected the tracts. If tracts conforming to the expected course of the SCP, middle cerebellar peduncle (MCP), or IPC were demonstrated, the reconstruction was considered successful. For tracts that were successfully demonstrated, we described the appearance as either symmetric or asymmetric between the right and left sides; a perceived difference of  $>25\%$  in length or the number of tracts between sides was considered asymmetric. Given the exploratory nature of this study, we did not perform quantitative analysis of lateral asymmetry because it could relate to technical parameters rather than biologic differences. For each peduncle, we recorded the tract volume, ADC, and FA. Using the temporal motion-tracking feature of the MT-SVR algorithm, we also recorded absolute motion data (millimeters) during the diffusion acquisitions.<sup>14</sup> We performed a subanalysis of the individual components of the MCP that have been described in prior postnatal tractography studies.<sup>22</sup> The subcomponents include those associated with cognitive (cognitive pathway of the MCP [MCP<sub>cog</sub>]) and motor and sensory (motor pathway of the MCP [MCP<sub>mot</sub>]) functions. The MCP<sub>cog</sub> was defined by the inferior and lateral tracts that extend from the rostral pons to the cerebellar hemispheres. The MCP<sub>mot</sub> was defined as the superior and medial tracts that extend from the caudal pons to the cerebellar hemispheres.<sup>22,23</sup>

### Statistical Analysis

Descriptive statistics summarized the demographic information and other categorical variables. The association between “low-quality data” and fetal position (breech or cephalic) was evaluated with a Fisher exact test. Similarly, differences in the frequency of rightward and leftward asymmetries as determined by qualitative inspection were evaluated using a Fisher exact test. Success in anatomic tract delineation, after excluding low-quality data, and its association with GA and motion were evaluated using Wilcoxon rank sum tests. A multiple linear regression analysis was used to evaluate tract-specific changes. We estimated the rate of change per week by evaluating GA as a predictor of volume, FA, and ADC for each anatomic tract (SCP, MCP, and ICP). Then, we performed an ANCOVA to compare the rate of change between tracts. STATA/SE, Version 15.1 (StataCorp) software was used to perform all analyses.

## RESULTS

### Sample Characteristics

Of 82 fetuses evaluated, 76 were in a cephalic position and 6 were in a breech position. A total of 24 fetuses could not be analyzed

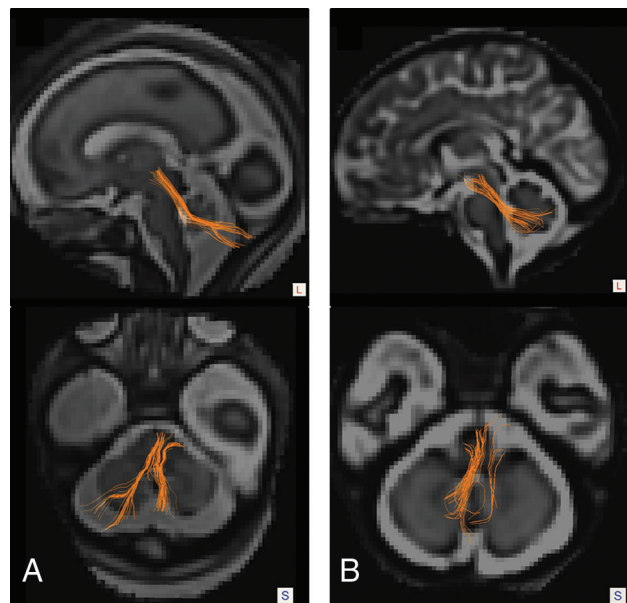


**FIG 1.** Tractography of the cerebellar peduncles in fetuses of varying gestational ages. Sagittal and axial tractography images overlaid on super-resolution T2 reconstructions show successful and symmetric delineation of the SCP in a 26-week 5-day-old male fetus (A). Sagittal and axial tractography images in a 36-week 2-day-old male fetus show successful tractography with asymmetry in the SCP reconstructions (B).

due to low-quality reconstruction/failure (see Online Table 1 for a list of failed cases and related artifacts). There was no association between tractography DTI reconstruction failure and fetal position ( $P = .570$ ). Of the 58 subjects in which tractography of DTI reconstruction was of acceptable quality, 38 were male, 19 were female, with the sex of 1 fetus unknown. The median GA was 30 weeks 4 days (interquartile range, 7 weeks). The youngest subject was 21 weeks 2 days, and the oldest subject was 37 weeks.

### Anatomic Analysis of Tracts

We identified the SCP (Fig 1) in 39 of 58 subjects (69%), of which 15 had symmetric tract representation. Of the 24 subjects with asymmetric SCPs, 13 (54.2%) had a rightward asymmetry and 11 (45.8%) had a leftward asymmetry ( $P = .683$ ). There was no significant difference in GA ( $P = .4420$ ) or absolute motion ( $P = .567$ ) between subjects with successful SCP tractography and those without successful delineation of the tract. Similarly, there were no significant differences in the GA ( $P = .520$ ) or absolute motion ( $P = .601$ ) between subjects with symmetric and asymmetric tract representation. A summary of GA and absolute motion metrics is available in Online Table 2.

The MCP was identified in all 58 subjects, and the reconstruction was symmetric in all (Fig 2). Distinct MCP<sub>cog</sub> and MCP<sub>mot</sub> were identified in 13 subjects (22%) (Fig 3). In subjects without a clear distinction of subcomponents, the MCP coursed inferiorly and laterally, extending from the rostral pons to the cerebellar hemispheres. There was no significant difference in GA ( $P = .520$ ) or absolute motion ( $P = .457$ ) between subjects with visualization of the 2 subcomponents versus those in which the subcomponents were not clearly distinct.

The ICP was not identified in any of the subjects analyzed.

### Age-Related Changes

There was a significant increase in tract volume with GA for the SCP (0.020 mL/week) and MCP (0.159 mL/week) (all,  $P < .05$ ) (Fig 4A). There was a significant difference ( $P < .001$ ) between linear regression models for the SCP and the MCP, with the MCP having, on average, greater volume than the SCP after controlling for GA. FA increased with GA for both the SCP (0.00685/week) and the MCP (0.00815/week) (all,  $P < .001$ ). The FA was significantly higher ( $P = .002$ ) for the MCP linear

regression model compared SCP after controlling for GA (Fig 4B). The ADC decreased with the GA for the SCP ( $-0.0000259 \text{ mm}^2/\text{s/week}$ ) and for the MCP ( $-0.0000253 \text{ mm}^2/\text{s/week}$ ) (all,  $P < .001$ ). The ADC was significantly lower ( $P < .001$ ) in the SCP linear regression model relative to the MCP after controlling for GA (Fig 4C).

### DISCUSSION

The motion artifacts of fetal MR imaging and the small size of the cerebellum have, until now, precluded the evaluation of fetal cerebellar microstructure with DTI. Using a recently introduced MT-SVR algorithm, we successfully performed DTI-based tractography of the SCP and MCP in 58 healthy second- and third-trimester fetuses and explored tract-specific developmental changes. By analyzing exclusively fetuses from normal pregnancies (with further confirmation on structural images at the time of the research scan), we minimized the risk of inadvertently introducing a bias into our analysis, which can occur when analyzing data from subjects referred for evaluation of suspected abnormalities. Our tractography analyses confirm a prenatal onset for differences in ADC, FA, and volume between the SCP and MCP and indicate that these differences arise as early as the second trimester. The MT-SVR reconstructions also enabled identification of distinct white matter bundles of the MCP in some subjects. The possibility of investigating tract-specific macro- and microstructural changes in the fetal cerebellar peduncles could improve our understanding of early functional specialization of the cerebellum, its selective vulnerability in the second half of pregnancy, and the complex neurologic sequelae associated with early cerebellar injury and developmental abnormalities.<sup>2-4,24,25</sup>

Prior studies using ex vivo high-angular-resolution diffusion imaging of fixed specimens showed the feasibility of performing tractography of the SCP, MCP, and ICP as early as the 17th week of postconceptional age.<sup>9,10</sup> The small size of the peduncles, the intricate posterior fossa anatomy, and artifacts related to fetal motion probably hindered these analyses on prior fetal tractography studies.<sup>26</sup>

Dovjak et al<sup>27</sup> had illustrated the cerebellar peduncles using DTI and tractography in a few individual fetuses, but a systematic analysis of developmental changes in these tracts has not been performed. The MT-SVR algorithm mitigates the motion artifacts by correcting the relative position of every diffusion section acquired, removing data affected by intraslice motion, and reconstructing the DTI with high spatial resolution, thereby addressing some of the major challenges mentioned above. The failure to identify the ICP likely reflects the small size and complexity of this tract, rather than limitations of the postprocessing algorithm, because prior reports on postnatal cerebellar tractography were unable to identify the ICP in infants younger than 2 months of age.<sup>22</sup>

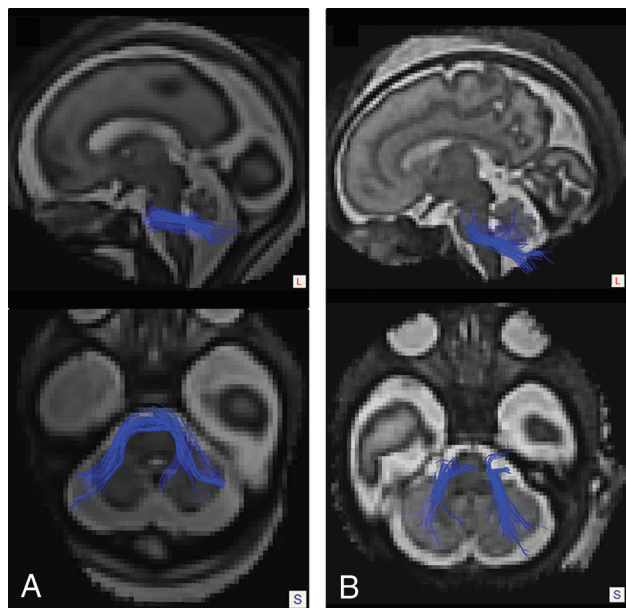


**FIG 2.** Tractography of the MCPs in fetuses of varying gestational ages. Sagittal and axial tractography images overlaid on super-resolution T2 reconstructions show successful and symmetric delineation of the MCP in a 26-week 5-day-old male fetus (A) and in a 33-week 6-day-old male fetus (B). Note symmetric representation of both tracts in the reconstructions.

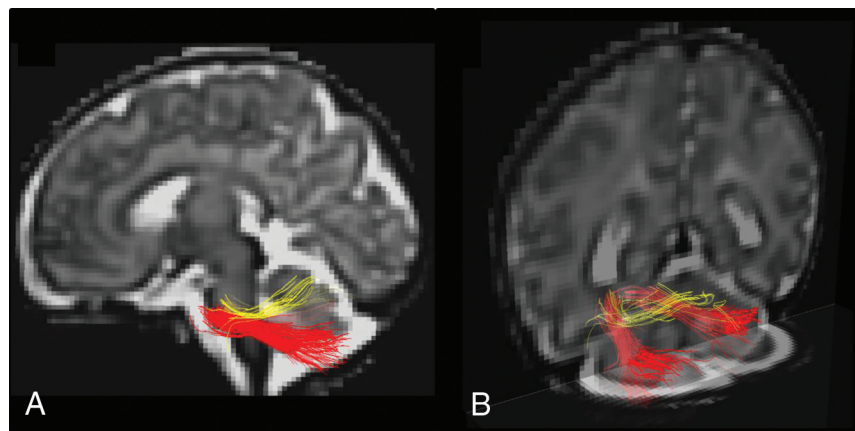


**FIG 3.** Tractography of the subcomponents of the MCP in a 36-week 2-day old male fetus. Sagittal (A) and posterior coronal oblique (B) tractography images overlaid on super-resolution T2 reconstructions show a clear distinction between the MCP<sub>cog</sub> (red) and the MCP<sub>mot</sub> (yellow). The MCP<sub>cog</sub> is larger and extends from the rostral pons to the lateral and inferior cerebellar hemispheres describing an oblique course. The MCP<sub>mot</sub> arises more caudally in the pons and extends toward the superior cerebellum, describing a more horizontal course.

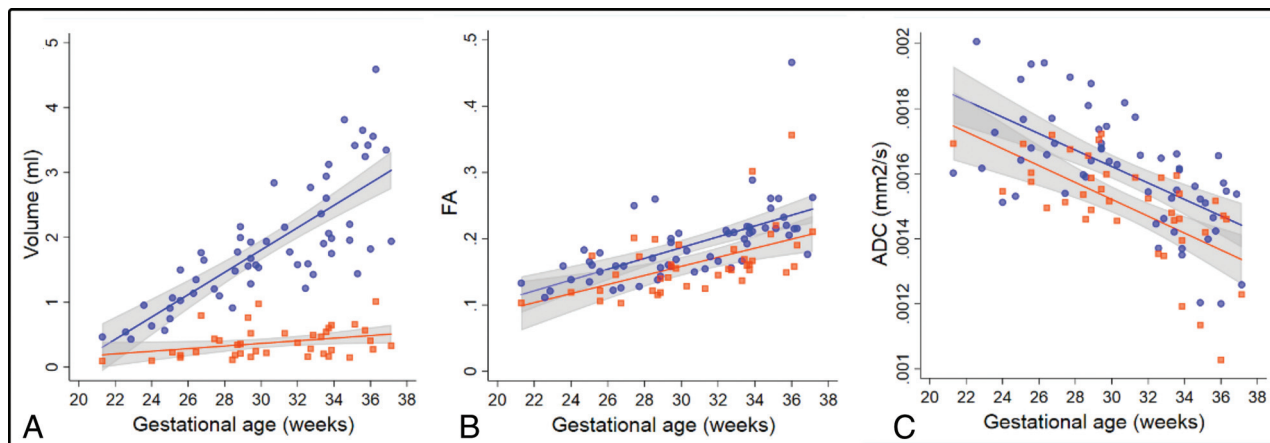


**FIG 4.** Changes in volume (A), FA (B), and ADC (C) for gestational age. Linear fit models are shown for the MCP (blue) and the SCP (orange), with their respective 95% confidence intervals (gray). Individual tract values for MCP (circles) and SCP (squares) are displayed.

The SCP followed its expected oblique course from the cerebellar hemispheres to the midbrain. In slightly more than half of the subjects, the tract appeared asymmetric, which we attribute to premature termination of the tractography driven by technical limitations. Artifacts in the fetal MR imaging, such as ghosting and low SNR from dielectric effects, are not homogeneously distributed across the image and are not mitigated by the MT-SVR algorithm, a feature that could result in some of the observed asymmetries. Considerations of spatial resolution and residual motion appear to be unrelated to these observations or play only a minor role because we did not find differences in GA or motion between subjects with symmetric and asymmetric reconstructions.

The anatomic details of the MCP tractography also correlated well with postnatal imaging and known neuroanatomy.<sup>22,28</sup> The MCP was seen in all subjects and always showed a symmetric reconstruction. The robustness of the reconstruction of this tract is at least, in part, the result of its larger size. The robust reconstruction of the MCP permitted identification of the MCP<sub>cog</sub> and MCP<sub>mot</sub> in approximately one-quarter of the fetuses. These distinct white matter bundles have been described in prior tractography studies postnatally and are thought to represent the cerebral and spinal components of the MCP (brachium pontis).<sup>23</sup>

We found significant age-related changes in ADC, FA, and volume in the SCP and MCP, which represent microstructural maturation and somatic growth. The rate of growth of the MCP outpaced that of the SCP; this trend is known to exist in early infancy, but our results confirm the prenatal onset of this divergence and suggest that it arises as early as the second trimester.<sup>22</sup> Re et al<sup>22</sup> reported that the MCP<sub>cog</sub> is the largest component of the MCP and that it grows faster than the MCP<sub>mob</sub>, though we did not perform volumetric analysis of these tracts due to the small sample size; subjective review of the tract morphology coincides with this description, with the MCP<sub>cog</sub> appearing larger than the MCP<sub>mot</sub> (Fig 3). Furthermore, in cases in which the individual tracts were not distinctly identified, the dominant configuration of the MCP appeared to follow that of the MCP<sub>cog</sub> fibers.

For both tracts, the ADC decreased with age and the FA increased with age, a finding that is frequently observed with progressing GA and postnatal age. Although there are significant differences in the absolute ADC and FA values between the 2 tracts, both exhibited fairly similar rates of change. Diffusion changes in the fetal white matter are the result of a complex series of cellular and compositional changes and are not solely explained by myelination. Back et al<sup>29</sup> and Zanin et al<sup>30</sup> characterized the series of events that occur with fetal white matter maturation using histology and imaging, respectively, including axonal organization, myelination gliosis, and ultimately myelin deposition. Some of these processes, such as myelination gliosis, are hypothesized to have a larger effect on ADC than on FA, whereas others, such as myelin deposition and axonal reorganization, are believed to influence both.<sup>29,30</sup>

A good example of the potential utility of tractography to enhance diagnosis is posterior fossa malformations such as Joubert syndrome.<sup>31</sup> While the morphologic findings of Joubert syndrome are readily apparent on postnatal imaging (small cerebellar vermis, thickened SCP with a horizontal configuration [molar tooth]), some of these may be difficult to identify in young fetuses, motion degraded scans, or oblique acquisitions. The lack of decussation of the SCP, a characteristic feature of Joubert syndrome, results in a unique parallel configuration on postnatal tractography that could help the radiologist identify the disorder with greater certainty in fetal MR imaging.<sup>32,33</sup> Tractography of the cerebellar peduncles and other posterior fossa tracts could also help in the identification of a variety of axonal guidance disorders (eg, tubulinopathies, pontine tegmental cap dysplasia), which are known to harbor aberrations in white matter connections.<sup>34,35</sup> Tractography could also improve our understanding of the emerging abnormalities in the fetal cerebellum in disorders such as congenital heart disease and intrauterine growth restriction, which are known to impact cerebellar development.<sup>6,36</sup> Even though the existing literature focuses on volumetric analysis of these structures, the distinct physiology of SCP and MCP could provide insights into the specific networks that have been affected, such is the case of long-term follow-up of white matter injury of prematurity, in which

abnormalities in the SCP correlate with motor outcomes and abnormalities in the MCP correlate with a lower intelligence quotient at 7 years of age.<sup>37</sup>

The current study has several limitations. First, we performed a qualitative analysis of only lateral asymmetry of the tracts analyzed. Given that there are still some limitations to the technique, including premature termination of fiber tracking, the complex trajectories of these tracts (decussate in the midline) and the inability to reliably evaluate crossing fibers with the diffusion tensor model, we consider that a potential quantitative analysis of lateral asymmetries was prone to type I and II errors, particularly given the absence of any difference on the qualitative analysis. Second, although we can infer some of the biologic mechanisms that underlie the change in diffusivity based on prior studies of histopathology, we do not have direct histologic correlation of these findings. Third, although the technique appears promising in studying normal cerebellar development and injury prenatally, additional studies testing specific clinical hypothesis are needed. Our diffusion MR imaging protocol involved repeat acquisitions with 12 gradient directions. In the presence of fetal motion that perturbed gradient directions, this scheme resembled a high-angular-resolution diffusion imaging protocol with jittered q-space samples on the sphere (with 1 b-value). Nonetheless, the relatively low spatial resolution of the fetal diffusion scans (compared with the small size of the fetal cerebellar structures) and residual motion artifacts reduced our ability to visualize and assess decussation of the SCP on color FA or tensor images in this study.

## CONCLUSIONS

Fetal DTI processed with a robust MT-SVR algorithm enabled deterministic tractography of the SCP and MCP in vivo. The reconstructions also permitted detailed characterization of tract-specific developmental changes in volume, ADC, and FA that set the trends for growth and maturation of these pathways in early postnatal life.

Disclosures: Fedel Machado-Rivas—RELATED: Grant: Research reported in this study was supported, in part, by the National Institute of Biomedical Imaging and Bioengineering and the National Institute of Neurological Disorders and Stroke of the National Institutes of Health Award Nos. R01EB018988, R01NS106030, and R01EB013248; a Technological Innovations in Neuroscience Award from the McKnight Foundation; a Schlaefer Fellowship for Neuroscience Research; and the Fetal Health Foundation. The content is solely the responsibility of the authors and does not necessarily represent the official views of the Fetal Health Foundation or the McKnight Foundation.\* Bahram Marami—RELATED: Grant: Research reported in this study was supported, in part, by the National Institute of Biomedical Imaging and Bioengineering and the National Institute of Neurological Disorders and Stroke of the National Institutes of Health under Award Nos. R01EB018988, R01NS106030, and R01EB013248; a Technological Innovations in Neuroscience Award from the McKnight Foundation; a Schlaefer Fellowship for Neuroscience Research; and the Fetal Health Foundation. The content is solely the responsibility of the authors and does not necessarily represent the official views of the National Institutes of Health, Fetal Health Foundation, or the McKnight Foundation.\* Caitlin Rollins—RELATED: Grant: National Institutes of Health/National Institute of Neurological Disorders and Stroke\*; UNRELATED: Expert Testimony: McCann Law, Comments: expert opinion writing; Grants/Grants Pending: National Institutes of Health, Children's Heart Foundation. Cynthia Ortin—RELATED: Grant: National Institutes of Health, Comments: National Institutes of Health/National Heart, Lung, and Blood Institute award No. K23HL141602.\* Simon Warfield—RELATED: Grant: National Institutes of Health.\* Ali Golipour—RELATED: Grant: National Institutes of Health, Comments: The imaging and image processing in this article was partly supported by grants from the National Institutes of Health\*; UNRELATED: Employment: Boston Children's Hospital and Worcester Polytechnic Institute, Comments: paid through employment as research and teaching faculty; Grants/Grants Pending: National Institutes of Health.\* \*Money paid to the institution.

## REFERENCES

- Volpe JJ. Cerebellum of the premature infant: rapidly developing, vulnerable, clinically important. *J Child Neurol* 2009;24:1085–104 [CrossRef Medline](#)
- Tarui T, Limperopoulos C, Sullivan NR, et al. Long-term developmental outcome of children with a fetal diagnosis of isolated inferior vermian hypoplasia. *Arch Dis Child Fetal Neonatal Ed* 2014;99:F54–58 [CrossRef Medline](#)
- Limperopoulos C, Bassan H, Gauvreau K, et al. Does cerebellar injury in premature infants contribute to the high prevalence of long-term cognitive, learning, and behavioral disability in survivors? *Pediatrics* 2007;120:584–93 [CrossRef Medline](#)
- Matthews LG, Inder TE, Pascoe L, et al. Longitudinal preterm cerebellar volume: perinatal and neurodevelopmental outcome associations. *Cerebellum* 2018;17:610–27 [CrossRef Medline](#)
- Shah DK, Anderson PJ, Carlin JB, et al. Reduction in cerebellar volumes in preterm infants: relationship to white matter injury and neurodevelopment at two years of age. *Pediatr Res* 2006;60:97–102 [CrossRef Medline](#)
- Olshaker H, Ber R, Hoffman D, et al. Volumetric brain MRI study in fetuses with congenital heart disease. *AJNR Am J Neuroradiol* 2018;39:1164–69 [CrossRef Medline](#)
- Bouyssi-Kobar M, Du Plessis AJ, McCarter R, et al. Third trimester brain growth in preterm infants compared with in utero healthy fetuses. *Pediatrics* 2016;138:e20161640 [CrossRef Medline](#)
- Hooker JD, Khan MA, Farkas AB, et al. Third-trimester in utero fetal brain diffusion tensor imaging fiber tractography: a prospective longitudinal characterization of normal white matter tract development. *Pediatr Radiol* 2020;50:973–83 [CrossRef Medline](#)
- Takahashi E, Song JW, Folkerth RD, et al. Detection of postmortem human cerebellar cortex and white matter pathways using high angular resolution diffusion tractography: a feasibility study. *Neuroimage* 2013;68:105–11 [CrossRef Medline](#)
- Takahashi E, Hayashi E, Schmahmann JD, et al. Development of cerebellar connectivity in human fetal brains revealed by high angular resolution diffusion tractography. *Neuroimage* 2014;96:326–33 [CrossRef Medline](#)
- Kasprian G, Del Río M, Prayer D. Fetal diffusion imaging: pearls and solutions. *Top Magn Reson Imaging* 2010;21:387–94 [CrossRef Medline](#)
- Chartier AL, Bouvier MJ, McPherson DR, et al. The safety of maternal and fetal MRI at 3T. *AJR Am Roentgenol* 2019;213:1170–73 [CrossRef Medline](#)
- Jaimes C, Delgado J, Cunnane MB, et al. Does 3-T fetal MRI induce adverse acoustic effects in the neonate? A preliminary study comparing postnatal auditory test performance of fetuses scanned at 1.5 and 3 T. *Pediatr Radiol* 2019;49:37–45 [CrossRef Medline](#)
- Marami B, Mohseni Salehi SS, Afacan O, et al. Temporal slice registration and robust diffusion-tensor reconstruction for improved fetal brain structural connectivity analysis. *Neuroimage* 2017;156:475–88 [CrossRef Medline](#)
- Khan S, Vasung L, Marami B, et al. Fetal brain growth portrayed by a spatiotemporal diffusion tensor MRI atlas computed from in utero images. *Neuroimage* 2019;185:593–608 [CrossRef Medline](#)
- Jaimes C, Machado-Rivas F, Afacan O, et al. In vivo characterization of emerging white matter microstructure in the fetal brain in the third trimester. *Hum Brain Mapp* 2020;41:3177–85 [CrossRef Medline](#)
- Jaimes C, Rofeberg V, Stopp C, et al. Association of isolated congenital heart disease with fetal brain maturation. *AJNR Am J Neuroradiol* 2020;41:1525–31 [CrossRef Medline](#)
- Kainz B, Steinberger M, Wein W, et al. Fast volume reconstruction from motion corrupted stacks of 2D slices. *IEEE Trans Med Imaging* 2015;34:1901–13 [CrossRef Medline](#)
- Marami B, Scherrer B, Afacan O, et al. Motion-robust diffusion-weighted brain MRI reconstruction through slice-level registration-based motion tracking. *IEEE Trans Med Imaging* 2016;35:2258–69 [CrossRef Medline](#)
- Wang R, Benner T, Sorensen AG, et al. Diffusion Toolkit: A Software Package for Diffusion Imaging Data Processing and Tractography.

[http://trackvis.org/faq/2007\\_ISMRM\\_diffusion\\_toolkit.pdf](http://trackvis.org/faq/2007_ISMRM_diffusion_toolkit.pdf). Accessed  
???????

21. Catani M, Thiebaut de Schotten M. **A diffusion tensor imaging tractography atlas for virtual in vivo dissections.** *Cortex* 2008;44:1105–32 [CrossRef Medline](#)
22. Re TJ, Levman J, Lim AR, et al. **High-angular resolution diffusion imaging tractography of cerebellar pathways from newborns to young adults.** *Brain Behav* 2017;7:e00589 [CrossRef Medline](#)
23. Voogd J, Ruigrok TJ. Cerebellum and precerebellar nuclei. In: ?????, *The Human Nervous System*. Elsevier; 2012:471–74
24. Semmel ES, Dotson VM, Burns TG, et al. **Posterior cerebellar volume and executive function in young adults with congenital heart disease.** *J Int Neuropsychol Soc* 2018;24:939–48 [CrossRef Medline](#)
25. Srivastava S, Prohl AK, Scherrer B, et al; TACERN Study Group. **Cerebellar volume as an imaging marker of development in infants with tuberous sclerosis complex.** *Neurology* 2018;90:e1493–50 [CrossRef Medline](#)
26. Kasprian G, Brugger PC, Schöpf V, et al. **Assessing prenatal white matter connectivity in commissural agenesis.** *Brain* 2013;136:168–79 [CrossRef Medline](#)
27. Dovjak GO, Brugger PC, Gruber GM, et al. **OC03.02: 3D fetal MRI visualisation of cerebellar white matter tracts.** *Ultrasound Obstet Gynecol* 2019;54:6–6 [CrossRef](#)
28. Bruckert L, Shpanskaya K, McKenna ES, et al. **Age-dependent white matter characteristics of the cerebellar peduncles from infancy through adolescence.** *Cerebellum* 2019;18:372–87 [CrossRef Medline](#)
29. Back SA, Luo NL, Borenstein NS, et al. **Arrested oligodendrocyte lineage progression during human cerebral white matter development: dissociation between the timing of progenitor differentiation and myelinogenesis.** *J Neuropathol Exp Neurol* 2002;61:197–211 [CrossRef Medline](#)
30. Zanin E, Ranjeva JP, Confort-Gouny S, et al. **White matter maturation of normal human fetal brain: an in vivo diffusion tensor tractography study.** *Brain Behav* 2011;1:95–108 [CrossRef Medline](#)
31. Poretti A, Boltshauser E, Loenneker T, et al. **Diffusion tensor imaging in Joubert syndrome.** *AJNR Am J Neuroradiol* 2007;28:1929–33 [CrossRef Medline](#)
32. Hsu CC, Kwan GN, Bhuta S. **High-resolution diffusion tensor imaging and tractography in Joubert syndrome: beyond molar tooth sign.** *Pediatr Neurol* 2015;53:47–52 [CrossRef Medline](#)
33. Widjaja E, Blaser S, Raybaud C. **Diffusion tensor imaging of midline posterior fossa malformations.** *Pediatr Radiol* 2006;36:510–57 [CrossRef Medline](#)
34. Jissendi-Tchofo P, Doherty D, McGillivray G, et al. **Pontine tegmental cap dysplasia: MR imaging and diffusion tensor imaging features of impaired axonal navigation.** *AJNR Am J Neuroradiol* 2009;30:113–19 [CrossRef Medline](#)
35. Grant PE, Im K, Ahtam B, et al. **Altered white matter organization in the TUBB3 E410K syndrome.** *Cereb Cortex* 2019;29:3561–76 [CrossRef Medline](#)
36. Polat A, Barlow S, Ber R, et al. **Volumetric MRI study of the intrauterine growth restriction fetal brain.** *Eur Radiol* 2017;27:2110–18 [CrossRef Medline](#)
37. Shany E, Inder TE, Goshen S, et al. **Diffusion tensor tractography of the cerebellar peduncles in prematurely born 7-year-old children.** *Cerebellum* 2017;16:314–25 [CrossRef Medline](#)